

The Characterization Of Secondary Electron Emitters For Use In Large Area Photo-Detectors

Slade J. Jokela†, Igor V. Veryovkin†, Alexander V. Zinovev†, Jeffrey W. Elam††, Qing Peng††, and Anil U. Mane††

†Materials Science Division, Argonne National Laboratory, 9700 S. Cass Ave., Building 200, Argonne Illinois 60439-4831

††Energy Systems, Argonne National Laboratory, 9700 S. Cass Ave., Argonne Illinois 60439

Abstract. The Large-Area Picosecond Photo-Detector Project is focused on the development of large-area systems to measure the time-of-arrival of relativistic particles with, ultimately, 1 pico-second resolution, and for signals typical of Positron-Emission Tomography (PET), a resolution of about 30 pico-seconds. Our contribution to this project is to help with identification and efficient fabrication of novel electron emitting materials with properties optimized for use in such detectors. We have assembled several techniques into a single ultra-high vacuum apparatus in order to enable characterization of both photocathode and secondary electron emission (SEE) materials. This apparatus will examine how photocathode quantum efficiency and SEE material electron yield correlate to surface chemical composition, state, and band structure. The techniques employed in this undertaking are X-ray photoelectron spectroscopy (XPS) for surface chemical composition, ultraviolet photoelectron spectroscopy (UPS) for the determination of band structure and surface work function, as well surface cleaning techniques such as argon-ion sputtering. To determine secondary electron emission yields and quantum efficiencies of detector materials, we use electron optics from a low energy electron diffraction (LEED) system whose set of hemispherical electrodes allows for efficient collection of secondary and photo electrons. As we gain a stronger insight into the details of mechanisms of electron emission from photocathodes and SEE materials, we will be able to lay a foundation for the larger collaborative effort to design the next generation of large-area photo-detectors. We present our preliminary results on the SEE materials from our as-yet completed characterization system.

Keywords: Secondary electron emission, Atomic Layer Deposition, Magnesium Oxide, Aluminum Oxide, XPS

PACS: 79.20.Hx, 79.20.La, 82.80.Pv

INTRODUCTION

The Large-Area Picosecond Photodetectors (LAPPD)¹ Project is a collaborative effort by several national labs, universities and small companies. Our three-year goal is to develop commercializable, lower-cost large-area detector systems capable of measuring the time of arrival of relativistic particles with 1 picosecond resolution and capable of measuring signals typical of positron-emission tomography (PET) with 30 picosecond resolution.

The Surface Chemistry group at Argonne National Laboratory (ANL) has been tasked with characterizing the thin film candidate materials for electron amplification (MgO and Al₂O₃) in the micro-channel plates that are being constructed for the LAPPD project, determining optimal film thickness and providing feedback on techniques intended to maximize secondary electron emission.

Secondary electron emission has been studied on a broad range of materials for many decades. The data from these experiments have been gathered in databases and reviewed extensively, showing that different studies on the same material rarely produce agreeing results. It has been known for quite some time that various differences in experimental instrumentation and conditions, as well as surface composition and morphology all play a role in a material's emission of secondary electrons.

EXPERIMENTAL SETUP

In order to further our understanding of the major contributing factors we are building at ANL an experimental apparatus for all-round characterization of emissive properties that includes Ultraviolet Photoelectron Spectroscopy (UPS), X-ray Photoelectron Spectroscopy (XPS), Ar-ion sputtering

for cleaning and film damage studies, and Secondary Electron Yield (SEY) measurements all in one Ultra-High Vacuum (UHV) chamber. While each of these techniques have been used before in conjunction with SEY characterization, to our knowledge, none have included them all in one UHV system, a necessity if one has to prevent changes in surface composition between measurements.

The surface composition of our samples is studied using XPS. Our XPS system implements a Mg K-alpha X-ray source (1253 eV) and a hemispherical electron energy analyzer (HA100 from VSW Scientific Instruments). The X-ray beam is neither collimated nor passed through a monochromator. However, the X-ray emission is narrow enough to obtain elemental composition as well as some chemical information from the samples. We intend to determine what correlations exist between surface composition and changes in band structure and surface work function using UPS. Our UPS system is comprised of a helium UV source and the aforementioned hemispherical analyzer. The primary operational mode of the UPS uses the He-I emission at 21.22eV (He-II emission is also possible). 5 keV Argon-ion sputtering, incident at approximately 45° to the sample surface, is used to remove surface contaminants and precursor molecules from the ALD process. While the removal of this material can be detected using XPS, it may also produce a change in the band structure, detectable by UPS. The SEY is measured using the electron gun from a Low Energy Electron Diffraction system (LEED, manufactured by Vacuum Generators) for a continuous-beam of fixed energy electrons, usually 950 eV for these experiments. Pulsed electron gun operation will be implemented in future studies. The electron beam had a diameter of about 1 mm with currents between 0.03 and 2.0 μA. The kinetic energy of the electrons is varied by applying a negative potential to the sample using a Keithley Source Meter instrument (Model 2410), which also samples the electrical current flow. The initial beam current, I_{beam} , is sampled by applying a positive 1100 Volt bias to the sample, preventing all secondary electrons from escaping the sample. We then vary the sample voltage from -950V to 0 V in one Volt increments, measuring the current flow at every point. The gain, γ , is then calculated using the following equation

$$\gamma = \frac{I_{collector}}{I_{beam}} = 1 - \frac{I_{sample}}{I_{beam}}, \quad (1)$$

where instead of using an external collector to collect the secondary electrons, we simply measure the

current flowing from the voltage source used to bias the sample, I_{sample} .

SAMPLE PREPARATION

This report details the findings on MgO and Al₂O₃ films fabricated by Atomic Layer Deposition (ALD)². These samples were deposited on boron-doped conductive-Si substrates and were prepared by the Energy Systems Division of ANL. ALD is ideally suited for the deposition of a conformal secondary emissive layer in the pores of micro-channel plates. More detail on the ALD technique can be obtained at the LAPPD Project website.¹ The samples used in the study of the effects of surface composition consisted of an Al₂O₃ film of thickness 113Å and an MgO film of thickness 290 Å. For our initial experiment studying how film thickness affects SE emission, a series of MgO films were created with thicknesses of 20, 30, 40, 55, 77, 110, and 200 Å. These samples were created together in the same growth run, limiting the chances of differences in sample composition and surface contamination due to ALD precursor molecules.

RESULTS

The Electron Dose Effect

Monitoring of the secondary electron yield as a function of primary electron energy showed a previously known effect that has been called the electron-dose effect.³ This effect is characterized by what is usually a decrease in secondary electron yield as a function of electron dose. We have monitored this effect in both Al₂O₃ and MgO. However, the results are drastically different for each material, showing the expected decrease in emission with dose for Al₂O₃ (Fig. 1) but showing an increase in emission with dose for MgO (Fig. 2). Exponential decay fits show that the SEY approaches 3.2 for Al₂O₃ and 9.0 for MgO.

During these experiments, the electron-beam current steadily increased from 0.05 to 0.15 μA. This change in current was slow enough that it did not affect the gathering of individual SEY curves, but over the course of 1.5 hours that yield data was collected, the current increase prevents us from analyzing current density effects. Future improvements to the system hardware as well as startup procedures will be made to stabilize beam current.

Prior experiments have shown that surface contaminants, such as carbon,⁴ can decrease electron yield. While these samples have been exposed to air between growth and characterization, allowing for CO₂ to chemisorb and dissociate on the surface,⁵ it has

also been suggested that in some materials, carbon can be stimulated to move to the surface from deeper within the sample.⁶

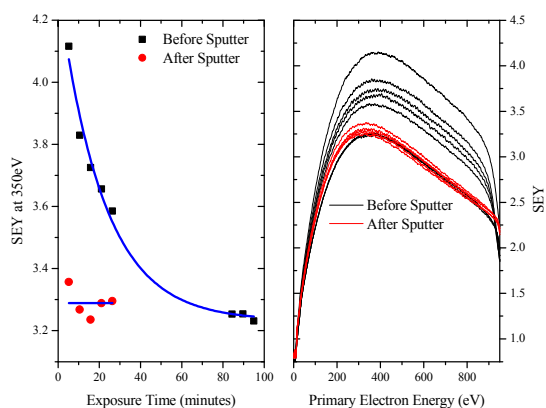


FIGURE 1. Secondary electron yield curves (right) for Al_2O_3 showing the electron-dose effect. The plot on the left shows emission at 350 eV as a function of exposure time. After Ar-ion sputtering, the emission stabilizes, presumably from the removal of a carbonaceous layer, observed in XPS spectra in Fig. 3.

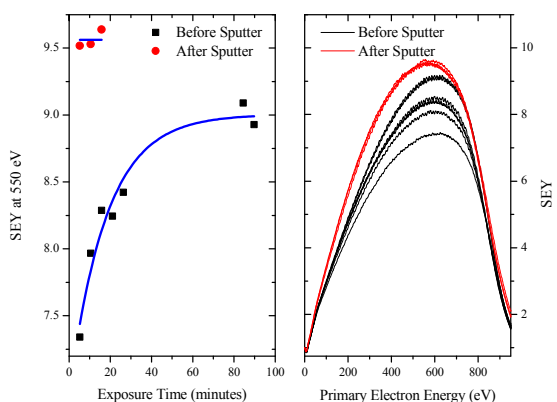


FIGURE 2. Secondary electron yield curves (right) for MgO showing the electron-dose effect (black). The plot on the left shows emission at 550 eV as a function of exposure time. After Ar-ion sputtering (red), the emission stabilizes, presumably from the removal of a carbonaceous layer, observed in XPS spectra in Fig. 4. Sample charging clearly present for higher primary electron energies, where the applied sample bias approaches 0V.

In our experiments, both Al_2O_3 and MgO films show carbon contamination in their XPS spectra (Figs. 3 and 4, respectively). This carbon is most likely from ALD precursor molecules and atmospheric contamination. Additionally, MgO shows a second carbon and oxygen peak. To determine whether these species are responsible for the dose effect observed on these samples, we sputter cleaned them using the 5keV

Ar-ion source. After sputter cleaning, the carbon peaks, as well as the extra oxygen peak for the MgO sample, were virtually eliminated. The simultaneous removal of the second carbon and oxygen peak on the MgO sample would indicate the presence of a C-O bond.

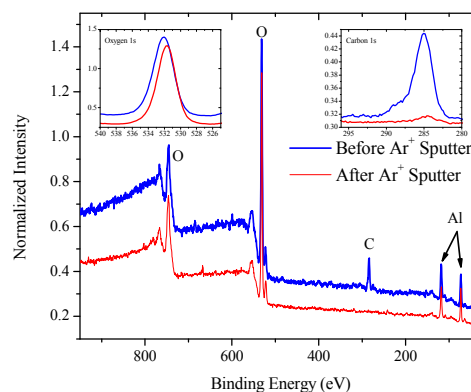


FIGURE 3. XPS spectra for Al_2O_3 before (blue) and after (red) Ar-ion sputtering. Spectra are normalized to the 532eV oxygen 1s peak height. The near-complete elimination of carbon appears to stabilize secondary electron emission.

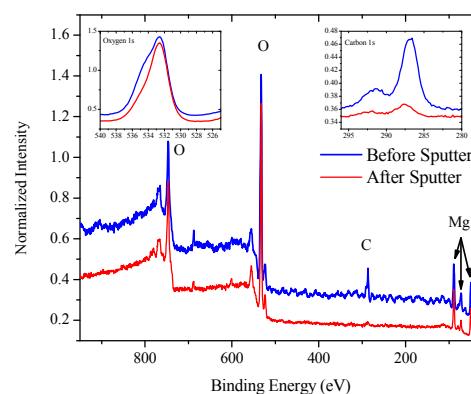


FIGURE 4. XPS spectra for MgO before (blue) and after (red) Ar-ion sputtering. Spectra are normalized to the 532eV oxygen 1s peak height. Of note is a second carbon and oxygen peak and their corresponding decrease in intensity after sputtering, indicating a C-O bond. This may be responsible for the difference in electron-dose effect between Al_2O_3 and MgO .

Observing the secondary electron emission in a different point on the sample after sputter cleaning revealed that in both cases, the emission was stabilized at their large-dose values, approximately 3.3 for Al_2O_3 and 9.6 for MgO .

The results indicate that the carbon surface contamination is responsible for the dose effect. Our results from samples prior to sputter cleaning seem to

indicate that carbon was being removed via electron-stimulated desorption, confirmed by the stabilization seen after Ar-ion sputter cleaning. However, what still remains unclear is why the carbon compounds affect the samples differently, increasing emission in Al_2O_3 and decreasing the emission in MgO prior to their removal. It's unlikely that this can simply be explained by the emission characteristics of the carbon itself. It's more likely that the carbon somehow changes the effective work function of the surface, lowering it in the case of Al_2O_3 and increasing it in the case of MgO. This assertion is backed up by the presence of a C-O bond on the MgO surface.

Secondary Electron Emission Vs. Film Thickness

We are also interested in determining the optimal film thickness for our secondary electron emission materials. So far, we have only tested MgO samples for this experiment. Prior work has been done on samples thicker than 100\AA .^{7,8} Their results show that electron-induced conduction from the excitation of electrons into the conduction band during secondary emission results in high emission for MgO. However, once the films reach thicknesses greater than the penetration depth of the primary electrons, the emission begins to decrease due to the resistance of the additional MgO film. In this case, sample charging occurs due to the lack of adequate compensation for the secondary electrons emitted from the material.

In our experiment we probe the range from 20 to 200 \AA . Each sample's secondary electron emission was monitored for 1.5 hours allowing the sample's emission to stabilize, accounting for the electron-dose effect. In the final comparison, only the final, stabilized SEY curve was used in the comparison between samples of different thickness. The results show quite clearly that sample charging is affecting the emission curves for higher electron energies and is more apparent for thicker samples. The charging is only noticeable for higher energy electrons due to the configuration of our system; at these energies the sample's bias potential is close to 0V, allowing the charge to pull the secondary electrons back into the sample.

From this, we have concluded that the optimal film thickness for maximum emission resides between 110 and 200 \AA (Fig. 5). This is in agreement with other findings showing the maximum escape depth of secondary electrons in MgO to be approximately 180 \AA .⁹ Additionally, XPS spectra show that at 55 \AA , the Si emission peak is no longer visible (Fig. 6). Any additional material will simply result in increased

charging due to the increased resistance and decreased compensation for the emitted secondary electrons.

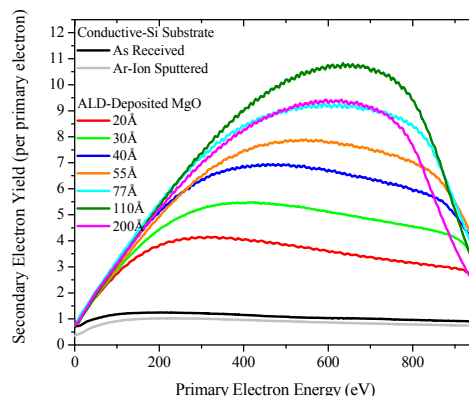


FIGURE 5. Secondary electron yield curves vs. MgO film thickness. The SEY increases until about 110 \AA where the emission begins to decrease.

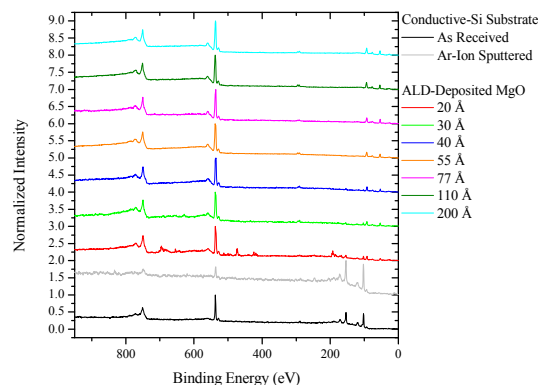


FIGURE 6. XPS Spectra corresponding to Fig. 5. The XPS spectra are normalized to the largest peak intensity (oxygen 1s, 532 eV, in all but the sputter cleaned Si sample). Of note are the Si peaks near 102 and 153 eV, which disappear with an MgO thickness of 55 \AA .

CONCLUSIONS

The SEY's dependence on electron dose for both alumina and magnesia films, known as the electron-dose effect, appears to be due to surface contamination. The difference in trend, decreasing SEY for Al_2O_3 and increasing SEY for MgO, could be a result of changes in the effective work function or band structure of the sample surface. This dose effect is eliminated once the sample is sputter cleaned.

Of the film-thicknesses tested, the sample of 110 \AA showed maximum secondary electron emission, in agreement with another study showing the maximum escape depth of secondary electrons to be

approximately 180 Å,⁹ others report it to be between 60 and 100 Å.¹⁰

Our future work will involve the continued enhancement of capabilities of our characterization system. We have plans to include pulsing operation of the electron beam to mitigate charging of the sample surface, providing us with more accurate SEY curves for insulating materials. Additional charge compensation techniques, such as increasing conductivity through sample heating, will also be explored. Furthermore, we have yet to fully implement the study of band structure using UPS, a crucial step in determining how surface contaminants affect the work function of the material. Finally, secondary neutral mass spectrometry (SNMS) is being considered for examination of molecules removed from the sample surfaces from electron stimulated desorption (ESD) as well as temperature programmed desorption (TPD). This will be used to confirm our findings that carbon is responsible for the electron-dose effect in our samples.

ACKNOWLEDGEMENTS

The submitted manuscript has been created by UChicago Argonne, LLC, Operator of Argonne National Laboratory (“Argonne”). Argonne, a U.S. Department of Energy Office of Science laboratory, is operated under Contract No. DE-AC02-06CH11357. The U.S. Government retains for itself, and others

acting on its behalf, a paid-up nonexclusive, irrevocable worldwide license in said article to reproduce, prepare derivative works, distribute copies to the public, and perform publicly and display publicly, by or on behalf of the Government. This work was supported in part by American Recover and Relief Act (ARRA) funds.

REFERENCES

1. The Large-Area Photodetector Project website <http://psec.uchicago.edu>.
2. George, S.M., Ott, A.W., and Klaus, J.W., *J. Phys. Chem* **100**, 13121 (1996).
3. Kumar, P., Watts, C., Gilmore, M., and Schamiloglu, E., *IEEE Trans. Plasma Sci.* **37**, 1537 (2009).
4. Kirby, R., “Instrumental effects in secondary electron yield and energy distribution measurements” at 31st *ICFA Advanced Beam Dynamics Workshop on Electron Cloud Effects*, 2004.
5. Ochs, D., Brause, M., Braun, B., Maus-Friedrichs, W., and Kempter, V., *Surf. Sci* **397**, 101 (1998).
6. Henrist, B., Hilleret, N., Scheuerlein, C., Taborelli, M., and Vorlaufer, G., in *The Proceedings of EPAC 2002, Paris, France, 2002*, pp. 2553.
7. Lee, J., Jeong, T., Yu, S., Jin, S., Heo, J., Yi, W., Jeon, D., and Kim, J.M., *Appl. Surf. Sci.* **174**, 62 (2001).
8. Meyza, X., Goeuriot, D., Guerret-Piécourt, Tréheux, D., and Fitting, H.-J., *J. Appl. Phys.* **94**, 5384 (2003).
9. Goldstein, B. and Dresner, J., *Surf. Sci* **71**, 15 (1978).
10. See, A. and Kim, W.S., *Appl. Phys. Letters* **81**, 1098 (2002).